Structural Characterization of Organocuprate Reagents. EXAFS Spectroscopy and *ab Initio* Calculations

Timothy L. Stemmler,† Terence M. Barnhart,† James E. Penner-Hahn,*,† Charles E. Tucker,‡ Paul Knochel,*,‡ Marlis Böhme,‡ and Gernot Frenking*,‡

Contribution from The Wiliard H. Dow Laboratories, Department of Chemistry, The University of Michigan, Ann Arbor, Michigan 48109-1055, and Fachbereich Chemie der Philipps-Universität Marburg, Hans-Meerwein-Strasse, 35043 Marburg, Germany

Received May 17, 1995®

Abstract: The cyanocuprate reagents, prepared from CuCN + 2 equiv of organolithium, appear to possess both unique spectroscopic and unique reactivity properties in comparison with the analogous reagents prepared from CuX (X = Cl, Br, I). We have used a combination of X-ray absorption near edge structure (XANES) and extended X-ray absorption fine structure (EXAFS) spectroscopies, together with *ab initio* structure calculations, to explore the structure of the Cu in these reagents. The XANES measurements support earlier, preliminary EXAFS indications that cyanide is not coordinated to Cu in the so-called "higher-order" cuprate prepared from CuCN + 2BuLi. Multiple scattering analyses of the EXAFS data have been used to characterize both the Cu−nearest neighbor and the Cu-outer shell interactions as a function of added organolithium. CuCN·2LiCl exists in THF as an oligomer of ···Cu-C≡N-Cu··· units. The average Cu environment consists of two coordinated cyanides with the possible presence of a third ligand for some of the Cu sites. CuCN + BuLi and CuCN + 2BuLi both contain two-coordinate Cu, with average Cu−C bond lengths of 1.89 and 1.93 Å, respectively. One cyanide remains coordinated to Cu in CuCN + BuLi, while both cyanides are displaced in CuCN + 2BuLi. *Ab initio* structure calculations are consistent with this picture, even to the extent of predicting the correct average Cu bond lengths. The theoretical calculations demonstrate that, in the most stable structure, the cyanide is associated with the alkyl groups that are bound to the Cu. This provides an explanation for the fact that, although the cyanide in CuCN + 2RLi is *not* coordinated to Cu, it nevertheless possess unique NMR properties. The cyanide−alkyl interaction may play a role in controlling the reactivity of the cyanocuprate reagents.

Organocopper compounds are versatile reagents for organic synthesis.[1−6] They are prepared by transmetalation of lithium, magnesium, or zinc organometallics, RM (M = Li, MgX or ZnX), with copper(I) salts, CuX.[1−8] The ratio of organometallic reagent (RM) to copper salt is crucial in determining the reactivity of the resulting copper species. Thus, lithium cuprates prepared by the addition of 2 equiv of RLi to a copper salt, commonly written as $R_2CuLi{\cdot}LiX$, display a greater reactivity than the corresponding organocopper reagent, RCu·LiX, prepared by using a 1:1 ratio of RLi and CuX.[1−6] In addition, the reactivity and the stability of the copper organometallic depends on the nature of the copper salt, CuX. Copper cyanide has been shown to give lithium cuprates that have remarkable stability and reactivity.[9−15] Thus, the coupling of $R_2CuLi{\cdot}LiCN$ with secondary alkyl iodides proceeds under extremely mild conditions (−50 °C, 0.5−1 h) and requires the use of only a small excess of organometallic reagent, while the analogous reaction using copper halides is quite difficult.[14] In an attempt to explain these reactivity differences, it has been suggested that "higher order" cuprates, $R_2Cu(CN)Li_2$, in which the copper atom is tricoordinated, are formed with CuCN but not with CuX (X = halide).[9−14] NMR investigations of solutions of these cuprates have led to conflicting conclusions concerning their structure.[16−19] Bertz and co-workers found that the ^{13}C NMR chemical shifts of several cuprates prepared from CuI and CuCN in THF were identical[18] and that, whereas a $^{13}C-^{13}C$ NMR coupling constant could be detected for the reagents formed from CuCN + RLi, no ^2J coupling between CN and C_1 could be detected in reagents prepared from CuCN + 2RLi.[19] These results suggested that the cyanide is not coordinated to the copper in "$R_2Cu(CN)Li_2$". However, Lipshutz and co-workers showed that the methyl signals from CuI + 2MeLi and CuCN + 2MeLi had different chemical shifts (>1 ppm) in Me_2S and that no free LiCN was present if MeLi was added to CuCN + MeLi.[16] These results were used to suggest that the cyanide and *both* of the methyl groups are coordinated to Cu in CuCN + 2MeLi.

The structures of a number of organocopper species have been determined by X-ray crystallography.[20−28] Unfortunately, no cyano-, organo-cuprate structures have yet been obtained. We

† The University of Michigan.
‡ Fachbereich Chemie der Philipps-Universität Marburg.
® Abstract published in *Advance ACS Abstracts*, December 1, 1995.

(1) Lipshutz, B. H.; Sengupta, S. *Org. React.* **1992**, *41*, 135.
(2) Normant, J. F.; Alexakis, A. *Synthesis* **1981**, 841.
(3) Posner, G. H. *Org. React.* **1972**, *19*, 1.
(4) Posner, G. H. *Org. React* **1975**, *22*, 253.
(5) Taylor, R. J. K. *Synthesis* **1985**, 364.
(6) Yamamoto, Y. *Angew. Chem., Int. Ed. Engl.* **1986**, *25*, 947.
(7) Knochel, P.; Singer, R. D. *Chem. Rev.* **1993**, *93*, 2117.
(8) Wipf, P. *Synthesis* **1992**, 537.
(9) Lipshutz, B. H. *Synlett* **1990**, 119.
(10) Lipshutz, B. H. *Synthesis* **1987**, 325.
(11) Lipshutz, B. H.; Wilhelm, R. S.; Kozlowski, J. A. *Tetrahedron* **1984**, *40*, 5005.
(12) Lipshutz, B. H.; Kozlowski, J.; Wilhelm, R. H. *J. Am. Chem. Soc.* **1982**, *104*, 2305.
(13) Lipshutz, B. H.; Wilhelm, R. S. *J. Am. Chem. Soc.* **1982**, *104*, 4696.
(14) Lipshutz, B. H.; Wilhelm, R. S.; Floyd, D. M. *J. Am. Chem. Soc.* **1981**, *103*, 7672.
(15) Bertz, S. H.; Dabbagh, G. *J. Chem. Soc., Chem. Commun.* **1982**, *18*, 1030−1032.
(16) Lipshutz, B. H.; Sharma, S.; Ellsworth, E. L. *J. Am. Chem. Soc.* **1990**, *112*, 4032−4034.
(17) Bertz, S. H.; Dabbagh, G. *J. Am. Chem. Soc.* **1988**, *110*, 3668.
(18) Bertz, S. H. *J. Am. Chem. Soc.* **1990**, *112*, 4031−4032.
(19) Bertz, S. H. *J. Am. Chem. Soc.* **1991**, *113*, 5470−5471.
(20) Hope, H.; Olmstead, M. M.; Power, P. P.; Sandell, J.; Xu, X. *J. Am. Chem. Soc.* **1985**, *107*, 4337−4338.

0002-7863/95/1517-12489$09.00/0

have recently reported preliminary structural data for lithium cyanocuprates based on extended X-ray absorption fine structure (EXAFS) spectroscopy.[29] On the basis of these data, we suggested that "higher order" cuprates are not formed from CuCN + 2BuLi. This conclusion was based on quantitative analysis of Cu-nearest neighbor ligand interactions and semi-quantitative analysis of the outer shell scattering. Herein, we report the complete analysis of the copper-ligand environment as determined by both EXAFS and X-ray absorption near edge structure (XANES). In addition, we report *ab initio* calculations which are consistent with the structures suggested by the EXAFS measurements.[29] Both the theoretical and experimental results strongly support our earlier conclusion that a three-coordinate copper unit, $R_2Cu(CN)^{2-}$, does not exist to any significant extent in cyanocuprate solutions.

Experimental Section

Sample Preparation. CuCN·2LiCl, 1.[30] CuCN (0.9 g, 10 mmol) and LiCl (ca. 0.84 g, 20 mmol; dried 2 h at 130 °C/0.1 mmHg) were dissolved in dry THF (50 mL) at 25 °C. A slightly yellow homogeneous solution was obtained after a few minutes of stirring at 25 °C.

BuLi·CuCN, 2.[31] A solution of BuLi (10 mmol, 1.6 M solution in hexanes) was added slowly at −70 °C to a suspension of CuCN (0.9 g, 10 mmol) in dry THF (ca. 50 mL). The reaction mixture was warmed until the dissolution of CuCN was observed (ca. −20 °C). The reaction mixture was cooled to −60 °C and was ready to use.

2BuLi·CuCN, 3.[10] A solution of BuLi (20 mmol, 1.6 M solution in hexanes) was added slowly at −70 °C to a suspension of CuCN (0.9 g, 10 mmol) in dry THF (50 mL). The reaction mixture was warmed until a homogeneous solution formed (ca. −30 °C).

Model Compounds. $NaCu(CN)_2 \cdot 2H_2O$ was prepared according to literature procedures.[32] All solid samples were prepared by grinding ca. 0.5 g of each solid with 1.5 g of boron nitride as an inert dilutant. $Zn(CN)_2$ and CuCN were purchased from Aldrich and used as received. EXAFS data for tricyano $K_2Cu(CN)_3$ (aq) complex was obtained from Prof. N. Blackburn.[33] These data were analyzed according to the protocol described below.

X-ray Absorption Measurements. X-ray absorption spectra were measured at 77 K at the Stanford Synchrotron Radiation Laboratory (SSRL) on beamline II-3, with synchrotron energies of 3.0 GeV and a stored current of 100 mA. These measurements were repeated at the National Synchrotron Light Source (NSLS) on beamline X9-A at 77 K with a synchrotron energy of 2.5 GeV and stored current of 200 mA. At SSRL, a Si(111) double-crystal monochromator was used. This was detuned by 50% for harmonic rejection. At NSLS, a Si-(220) double-crystal monochromator was used in conjunction with a harmonic rejection mirror. Both monochromators were calibrated using a Cu foil internal standard with the first inflection point of the foil defined as 8980.3 eV. All spectra were collected in transmission mode using ionization chambers filled with nitrogen gas. Cryogenic temperatures were maintained by placing the sample in thermal contact with a liquid nitrogen reservoir. Frozen solution and solid samples were placed in Al cells with mylar windows. Samples were prepared as described above and kept at 77 K for the duration of the experiment. All spectra were recorded from 8670 to 10 100 eV with a step size of 5 eV in the pre-edge (8650−8955 eV), 0.25 eV in the edge (8955−9004), and 0.05 $Å^{-1}$ in the EXAFS region (9004−9675 $Å^{-1}$). Integration times varied from 1 s in the pre-edge and edge regions to 15 s at $k = 13$ $Å^{-1}$ for a total scan time of ca. 35 min. In both cases the beam size was 2 × 12 mm^2. Two or three spectra were collected and averaged for each sample.

Data Analysis. The XAS spectra from each synchrotron were processed independently. Data analysis was performed according to established methods.[34] Edge data were normalized by fitting the smoothly varying parts of the absorption spectrum both below (8700−8950 eV) and above the edge (9005−9675 eV) to tabulated X-ray cross-sections, using a single polynomial background and scale factor. The EXAFS data were converted to k space using an initial E_0 value of 9000 eV (Cu) or 9675 eV (Zn) and were weighted by k^3 in order to compensate for the decreased EXAFS amplitude at high k. The EXAFS signal $k^3\chi(k)$ vs k was truncated at 2.5 and 12.5 $Å^{-1}$ and then Fourier transformed. The data were Fourier filtered to isolate the contributions corresponding to each peak in the Fourier transform. The best-fit bond lengths, coordination numbers, and Debye−Waller factors were determined from fitting both the unfiltered and Fourier filtered data using both empirical and theoretical amplitude and phase functions. The theoretical EXAFS parameters were obtained using *ab initio* calculations (FEFF v. 5.04) which account for multiple scattering interactions.[35−37] The correct scale factor and threshold energy (E_0) for the theoretical parameters were determined by fitting the EXAFS data for crystallographically characterized two- and three-coordinate Cu(I) complexes. The optimum scale factor and E_0 were 0.82 and 8991.15 eV. Empirical amplitude and phase functions were obtained from the EXAFS data for the crystallographically characterized[38] model $Zn(CN)_2$. In this case, the relative scale factor was 1.0, which amounts to assuming that the identity of the absorber has no effect on the EXAFS amplitude. The change in relative threshold energy from Zn to Cu was −10 eV, as determined by fits to Cu models. This ΔE_0 is consistent with the empirical difference in the edge energies (665 eV) vs the E_0 definition (9000 vs. 9675 eV) between Cu and Zn. When fitting unknown compounds, only the bond length and Debye−Waller factor for each shell were allowed to vary while the coordination number was systematically increased in half-integer steps from 0 to 6. For all of the systems studied, a single absorber/scatter interaction was sufficient to describe each shell of scatterers, i.e., each peak in the Fourier transform, although for **1**, inclusion of a second shell of nearest neighbors significantly improved the fit (see below).

Theoretical Methods. The geometries of the cuprates were optimized at the MP2/II (Møller−Plesset perturbation theory[39,40] terminated at second order) level of theory using an effective core potential (ECP)[41] for copper and all-electron basis sets for the other atoms. The $3s^2$ and $3p^6$ electrons were calculated explicitly as part of the Cu "valence" electrons. The valence basis set of Cu has [441/2111/41] quality, while a 6-31G(d) all-electron basis set[42−44] was used for the other atoms. This basis set combination is termed basis set II. Calculations at the MP2/II level of theory have been found to give

(21) Nobel, D.; van Koten, G. A.; Slpek, L. *L. Angew. Chem., Int. Ed. Engl.* **1989**, *28*, 208.
(22) van Koten, G.; Jastrezebski, T. B. H.; Muller, F.; Stam, C. H. *J. Am. Chem. Soc.* **1985**, *107*, 697.
(23) Power, P. P. *Prog. Inorg. Chem.* **1991**, *39*, 75−112.
(24) Olmstead, M. M.; Power, P. P. *J. Am. Chem. Soc.* **1989**, *111*, 4135−4136.
(25) Hope, H.; Oram, D.; Power, P. P. *J. Am. Chem. Soc.* **1984**, *106*, 1149−1150.
(26) Olmstead, M. M.; Power, P. P. *J. Am. Chem. Soc.* **1990**, *112*, 8008.
(27) Lorenzen, N. P.; Weiss, E. *Angew. Chem., Int. Ed. Engl.* **1990**, *29*, 300−302.
(28) Leoni, P.; Pasquali, M.; Ghilardi, C. A. *J. Chem. Soc., Chem. Commun.* **1983**, 240−241.
(29) Stemmler, T. S.; Penner-Hahn, J. E.; Knochel, P. *J. Am. Chem. Soc.* **1993**, *115*, 348−350.
(30) Knochel, P.; Yeh, M. C. P.; Berk, S. C.; Talbert, J. *J. Org. Chem.* **1988**, *53*, 2392.
(31) Hamon, L.; Levisalles, J. *J. Organomet. Chem.* **1983**, *251*, 133.
(32) Kappenstein, C.; Hugel, R. P. *Inorg. Chem.* **1977**, *16*, 250−254.
(33) Han, J.; Blackburn, N. J.; Loehr, T. M. *Inorg. Chem.* **1992**, *31*, 3223−9.
(34) Teo, B. K. *EXAFS: Basic Principles and Data Analysis*; Springer-Verlag: New York, 1986; Vol. 9.
(35) Rehr, J. J.; Albers, R. C.; Natoli, C. R.; Stern, E. A. *J. Phys., Colloq.* **1986**, *1*, C8/31−C8/35.
(36) Rehr, J. J.; Mustre, d. L. J.; Zabinsky, S. I.; Albers, R. C. *J. Am. Chem. Soc.* **1991**, *113*, 5135−40.
(37) Rehr, J. J.; Albers, R. C.; Zabinsky, S. I. *Phys. Rev. Lett.* **1992**, *69*.
(38) Hoskins, B. F.; Robson, R. *J. Am. Chem. Soc.* **1990**, *112*, 1546−1554.
(39) Møller, C.; Plesset, M. S. *Phys. Rev.* **1934**, *46*, 618.
(40) Binkly, J. S. *Intern. J. Quantum Chem* **1975**, *9*, 229.
(41) Hay, P. J.; Wadt, W. R. *J. Chem. Phys.* **1985**, *82*, 299.
(42) Hehre, W. J.; Ditchfield, R.; Pople, J. A. *J. Chem. Phys.* **1972**, *56*, 2257.
(43) Hariharan, P. C.; Pople, J. A. *Theor. Chim. Acta* **1973**, *28*, 213.
(44) Pietro, W. J.; Francl, M. M.; Hehre, W. J.; Defrees, D. J.; Pople, J. A.; Binkley, J. S. *J. Am. Chem. Soc.* **1982**, *104*, 5039.

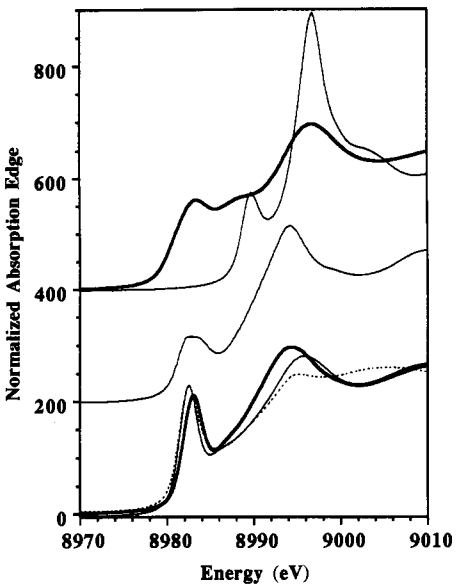

Figure 1. Normalized XANES spectra. (Bottom) spectra for solutions of **1** (bold line), **2** (light line) and **3** (dashed line). (Middle) XANES spectrum for $NaCu(CN)_2 \cdot 2H_2O$, in which each Cu is coordinated to three CN ligands. (Top) reference XANES spectra for CuCN (s) (bold line) and $Zn(CN)_2$ (s) (light line). Spectra offset vertically by +200 or +400 for clarity. Spectrum for $Zn(CN)_2$ (s) shifted by −665 eV.

very accurate geometries for Cu compounds[45] and other transition model complexes.[46,47] A set of five primitives was employed for the d-type polarization functions. The vibrational frequencies were calculated using numerical second derivatives. All calculations were carried out using the program package Gaussian 92.[48]

Results

XANES Data. Normalized XANES spectra for **1**−**3** are shown in Figure 1 (bottom). All three edges show intense pre-edge transitions at ca. 8982 eV. This has been assigned as a 1s → 4p transition.[49] The intensity of this feature decreases as complexes go from two to three to four coordinate, presumably as a result of increased Cu 4p + ligand orbital overlap. The intensity of 1s → 4p transition is identical for **2** and **3**, while this feature is slightly weaker in **1**. This decrease suggests a small increase in the average Cu coordination number for **1** relative to **2** and **3**. For reference, the XANES spectrum for $NaCu(CN)_2 \cdot 2H_2O$, in which each Cu is coordinated to three cyanides, is shown in Figure 1 (middle). It is clear that the 1s → 4p transition in this case is decreased significantly relative to those in **1**−**3**.

In addition to the 1s → 4p transition, the spectrum for **1** shows an intense continuum resonance at ca. 8995 eV. A similar transition is seen in the XANES spectra for authentic metal cyanides (see Figure 1, top and middle). We attribute this to a multiple-scattering resonance involving the linear M−C−N linkage, as illustrated by the intense edge feature seen for four-coordinate cyanide ligand environment for $Zn(CN)_2$. The intensity of this transition for **1** is comparable to that seen in solid CuCN, suggesting that the Cu in **1** is coordinated primarily

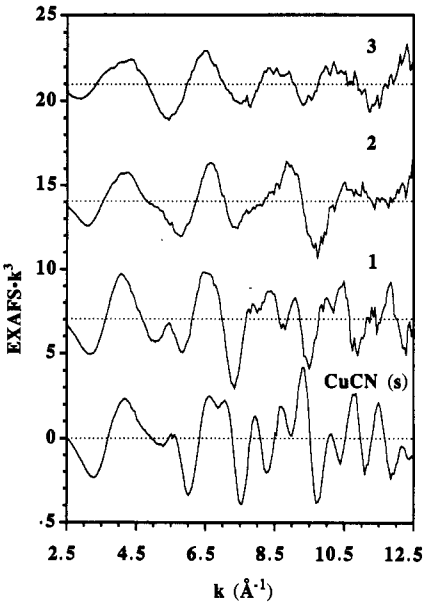

Figure 2. Unfiltered k^3 weighted EXAFS data for CuCN(s), **1**, **2**, and **3**. The spectra for **1**, **2**, and **3** have been offset vertically by 7, 14, and 21, respectively, for clarity.

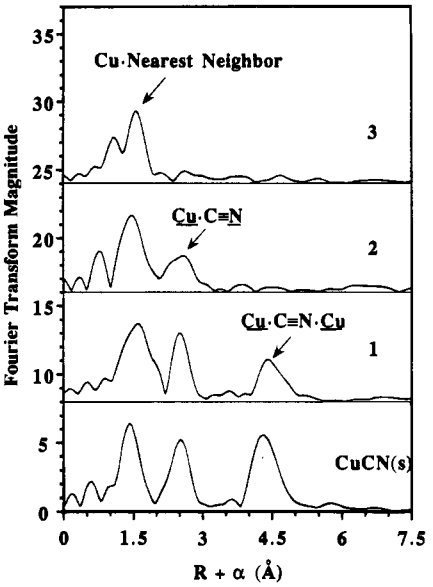

Figure 3. Fourier transform of the EXAFS data for **1**, **2**, **3**, and CuCN-(s) calculated using k^3 weighted EXAFS from $k = 2.5-12.5$ Å^{-1}. The spectra for **1**, **2**, and **3** have been offset vertically by 8, 16, and 24, respectively, for clarity.

to cyanide ligands. The intensity of the 8995 eV transition decreases from **1** to **2** to **3**, suggesting a progressive loss of cyanide ligands as BuLi is added.

EXAFS Data. The EXAFS data for **1**, **2**, **3**, and CuCN (s) are compared in Figure 2. The spectra for CuCN (s) and **1** are quite complex, demonstrating that there must be substantial long-range order in these materials. As the ratio of BuLi to CuCN is increased, the higher frequency oscillations disappear, indicating a loss of long-range order in **2**, and particularly in **3**. Figure 3 shows the Fourier transforms of these EXAFS spectra. The Fourier transform of an EXAFS spectrum gives a pseudoradial distribution function around the absorbing atom (Cu). Peak positions in the Fourier transform are shifted by ~−0.4 Å relative to the true Cu-scatterer distances. The spectra for both CuCN (s) and **1** show three principal features above the noise level (the noise level can be estimated from the amplitude of the Fourier transform at $R + \alpha > \sim 6$ Å). These three peaks,

(45) Böhme, M.; Frenking, G.; Reetz, M. T. *Organometallics* **1994**, *13*, 4237.
(46) Ehlers, A. W.; Frenking, G. *Organometallics* **1995**, *14*, 423.
(47) Ehlers, A. W.; Frenking, G. *J. Am. Chem. Soc.* **1994**, *116*, 1514.
(48) Frisch, M. J.; Trucks, G. W.; Head-Gordon, M.; Gill, P. M. W.; Wong, M. W.; Foresman, J. B.; Schlegel, H. B.; Raghavachari, K.; Robb, M. A.; Binkley, J. S.; Gonzalez, C.; Martin, R.; Fox, D. J.; DeFrees, D. J.; Baker, I.; Stewart, J. J. P.; Pople, J. A. Gaussian 92; Gaussian, Inc.: Pittsburgh, PA, 1992.
(49) Kau, L. S.; Spira, S. D. J.; Penner, H. J. E.; Hodgson, K. O.; Solomon, E. I. *J. Am. Chem. Soc.* **1987**, *109*, 6433−42.

Table 1. Curve Fitting Results for Unfiltered Cyanocuprate EXAFS[a]

	Cu−C[b]			Cu···N[c]			Cu···Cu[d]			
sample	R (Å)	CN	σ^{2f}	R (Å)	CN	σ^{2f}	R (Å)	CN	σ^{2f}	model[e]
CuCN (s)	1.85	2.0	1.3	3.04	2.0	1.2	4.89	2.0	1.9	$Zn(CN)_2$
	1.86	2.0	1.4	3.01	1.5	3.3	4.87	1.0	3.8	CuCN (th)
1	1.96	3.0	1.0	3.09	2.0	1.3	5.01	2.0	2.0	$Zn(CN)_2$
	1.97	2.5	3.2	3.05	1.5	4.1	4.99	1.0	6.6	CuCN (th)
2	1.89	2.0	0.6	3.10	1.5	1.5				$Zn(CN)_2$
	1.90	2.0	2.8	3.07	1.0	4.1				CuCN (th)
3	1.93	2.0	1.2							$Zn(CN)_2$
	1.94	2.0	3.4							CuCN (th)
$Cu(CN)_3^{2-}$	1.93	3.0	1.3	3.13	3.0	3.7				$Zn(CN)_2$
	1.94	3.0	1.4	3.10	3.0	4.1				CuCN (th)
	1.93	*3.0*	*3.09*	*3.0*						*g*

[a] Values reported are the averages for duplicate data sets. Estimated accuracy is as follows: R (absorber−scatterer distance), ±0.02 Å for first shell, ±0.05 Å for outer shell; CN (coordination number), ±0.5; σ^2 (Debye−Waller factor), ± 2 × 10^{-3} Å^2 based on studies of model compounds. The reproducibility from sample to sample is considerably better than this: R ± 0.005 Å, CN ± 0.25, σ^2 ± 0.8 × 10^{-3} Å^2. Data fit over a k range of 2.5 to 12.5 Å^{-1}. [b] Cu−C nearest neighbors. [c] *Cu*−C−*N* next nearest neighbors. [d] *Cu*−C−N−*Cu* outer shell scattering. [e] EXAFS were fit both with empirical parameters derived from $Zn(CN)_2$ (s) and with theoretical parameters derived from a Cu−C≡N−Cu model. It is not possible to distinguish between Cu−C, Cu−N, and Cu−O scattering in EXAFS. [f] Debye−Waller factor × 10^3 in units of Å^2. For the theoretical parameters, this represents an absolute Debye−Waller factor. For the empirical parameters, this gives the change in Debye−Waller factor relative to $Zn(CN)_2$. [g] Crystallographic distances for $Na_2Cu(CN)_3 \cdot 3H_2O$ (ref 52).

at $R + \alpha \sim 1.5$, 2.5, and 4.3 Å, are attributed to *Cu*−*C* nearest neighbors ($R \sim 1.9$ Å), *Cu*−C−*N* next nearest neighbors ($R \sim 3$ Å) and *Cu*−C−N−*Cu* distant scattering ($R \sim 5$ Å), respectively. Thus, from the Fourier transform alone it is apparent that there is substantial oligomerization in both CuCN (s) and **1**. The Fourier transform for **2** retains the features at 1.5 and 2.5 Å. However, the feature at 4.5 Å is noticeably absent. The Fourier transform for **3** shows only a nearest neighbor peak at ~1.5 Å. Thus, no significant long-range order is observed for this solution.

Multiple Scattering. Multiple scattering refers to the situation in which the X-ray excited photoelectron is scattered by two or more scatterers before returning to the absorbing atom. For example, in the system M−A−B, the photoelectron may go either M → B → M (single scattering) or M → A → B → M (multiple scattering). Multiple scattering is most important for linear M−A−B systems and becomes negligible when the M−A−B angle is less than ~150°.[50] The most important consequence of multiple scattering is that the photoelectron wave is focused by the intervening atom (A in the example above) toward the outer scattering atom (B). This leads to a significant enhancement in the apparent back-scattering amplitude for atom B. In addition, an extra phase shift, introduced by the intervening atom A, causes a decrease in the apparent M···B distance.

Multiple scattering is important in the EXAFS of the linear cyanide groups in $Zn(CN)_2$ and $Cu(CN)_3^{2-}$.[51,52] The Fourier transforms for both $Zn(CN)_2$ and CuCN show large peaks at $R + \alpha \sim 4.5$ Å (see Figure 4). In the former, this can be assigned with confidence to *Zn*−C−N−*Zn* EXAFS since the crystal structure of $Zn(CN)_2$ is known.[38] By analogy, we attribute the corresponding peaks in CuCN to *Cu*−C−N−*Cu* scattering. EXAFS scattering normally falls off as $1/R^2$; thus, it is unusual to observe peaks of this intensity arising from such long-distance interactions. In both cases, we attribute the detectability of the M···M EXAFS to strong multiple scattering through an intervening linear cyanide. Multiple scattering calculations on the linear Cu−C≡N−Cu system are consistent with this interpretation (see Figure 4). Although the outer shell peaks in this simulation are somewhat more intense than those in the experimental spectrum, the positions of the peaks show excellent agreement. The excess intensity most likely reflects a failure to account for increasing disorder as the absorber−scatterer distance increases.

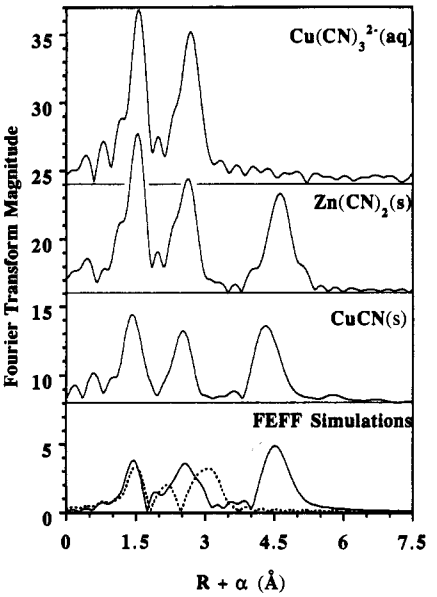

Figure 4. Fourier transform of the EXAFS data. (Bottom) theoretical simulations of the EXAFS for a linear Cu−C≡N−Cu model (solid line) and μ-1,1-CN bridging model (dashed line) with a Cu−C−Cu angle = 120°. (Top) experimental spectra for CuCN (s), $Zn(CN)_2$ (s), and $Cu(CN)_3^{2-}$ (aq). EXAFS data were k^3 weighted over the k range of 2.5−12.5 Å^{-1}. Experimental spectra are offset vertically by 8, 16, and 24 for clarity.

In contrast with the excellent agreement found for a linear Cu−C≡N−Cu model, a hypothetical Cu(μ-1,1-CN)Cu geometry does not account for the observed EXAFS (dashed line in Figure 4). The Cu···N and Cu···Cu peaks occur at significantly shorter distances and with approximately one-half the amplitude in the μ-1,1-bridging geometry.

Fitting Analysis. EXAFS data for **1**, **2**, **3**, and CuCN (s) were fit both using empirical phase and amplitude parameters, obtained from $Zn(CN)_2$ (s), and using theoretical phase and amplitude parameters. Table 1 summarizes the fitting results obtained for both sets of parameters. For **2**, **3**, and CuCN (s), a single shell of low-Z nearest neighbors was sufficient to model the EXAFS contributions that give rise to the first Fourier

(50) Hedman, B.; Co, M. S.; Armstrong, W. H.; Hodgson, K. O.; Lippard, S. J. *Inorg. Chem.* **1986**, *25*, 3708−3711.
(51) Inoue, M. B.; Machi, L.; Inoue, M.; Fernando, Q. *Inorg. Chim. Acta* **1992**, *192*, 123.
(52) Kappenstein, C.; Hugel, R. P. *Inorg. Chem.* **1978**, *17*, 1945−9.

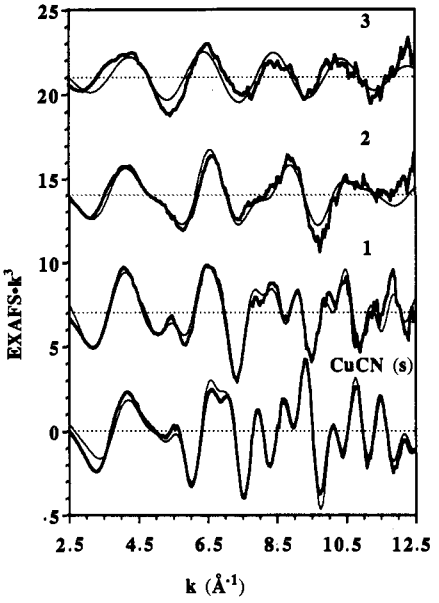

Figure 5. Best fits to unfiltered EXAFS data for CuCN(s), **1**, **2**, and **3** using a theoretical Cu−C≡N−Cu model. For each spectrum, the empirical data is shown as a bold line, with the best fit shown as a light line. Spectra for **1**, **2**, and **3** are offset vertically by 7, 14, and 21, respectively, for clarity.

transform peak. There was no evidence for a high-Z (e.g., Cl) scatterer in the EXAFS, and inclusion of a second shell of nearest neighbor scatterers did not improve the fit significantly. For **1**, a single shell of Cu−C scatterers could also be used to fit the data. In this case, however, there was a significant improvement in the fit quality if an additional shell of Cu−Cl scatterers was also included, with a Cu−Cl distance of approximately 2.2 Å.

For **3**, a single Cu−C environment adequately reproduced the EXAFS (see Figure 5). However, for **1**, **2**, CuCN(s), and $Cu(CN)_3^{2-}$ (aq), additional shells of scatterers were required. For **2** and $Cu(CN)_3^{2-}$ (aq), addition of a second shell of Cu···N was sufficient to fit the data, while for **1** and CuCN(s), a third shell of Cu···Cu was also necessary, as anticipated from the Fourier transforms. Essentially identical results were obtained for fits with the empirical $Zn(CN)_2$ parameters or with the *ab initio* parameters, although the empirical parameters appear to consistently overestimate the Cu···N and Cu···Cu distances relative to the *ab initio* parameters. For $Cu(CN)_3^{2-}$ (aq), where a crystal structure of the Na salt is available for comparison,[52] the *ab initio* parameters give a more accurate Cu···N distance. For most of the discussion, it is the *differences* in the outer shell distance that are important; thus, the small systematic deviations between the parameter sets are unimportant. Where absolute distances are needed, we will use the *ab initio* parameter set. Figure 5 shows the best fits to the EXAFS data for **1**, **2**, **3**, and CuCN(s).

Theoretical Results. In order to give additional information about the structures of the lower-order and higher-order cuprates, we carried out *ab initio* calculations of model compounds. In these calculations, the butyl substitutents have been replaced by methyl groups, because otherwise the molecules would be too big for optimization at the MP2/II level of theory. We do not expect that the relative energies of the isomers are significantly influenced by this alteration of the substituents. Figure 6 shows the optimized geometries and relative energies of the cyanocuprates **M1**−**M7**. Some of these compounds have previously been calculated by Snyder and co-workers.[53,54] Their results are very similar to our data.

The optimized geometry of the parent cuprate anion $MeCu(CN)^-$ (**M1**) has a linear structure. The calculated Cu−CN bond length (1.887 Å) is in excellent agreement with the experimental value (1.86 Å) for the Cu−nearest neighbor distance in CuCN (s). The average Cu−C distance in **M1** is 1.915 Å, in good agreement with the average Cu−C nearest-neighbor interaction deduced from the EXAFS data for **2** (1.90 Å).

The neutral structure **M2** has a linear energy minimum form **M2a** with slightly shorter Cu−C bonds than **M1**. However, monomeric **M2** has an energetically lower lying isomer **M2b**, which has the Li atom bridging the cyano moiety (Figure 6). It should be noted that the global energy minimum form of monomeric LiCN is also predicted to have a bridged (cyclic) geometry.[55] Structure **M2b** is 2.3 kcal/mol lower in energy than **M2a**. It is possible that **M2** has a linear structure in the condensed phase. The Cu−C distances of the bridged structure **M2b** are not very different from the optimized geometry of **M2a**.

We optimized several structural isomers of the 2:1 model lithium cuprate with a dicoordinate copper **M3** (Figure 6). The isomeric form **M3a**, which has the copper atom bound to the cyano moiety, is a minimum on the potential energy surface ($i = 0$). However, the isomeric forms **M3d** and **M3e**, which have no Cu−CN bonds, are clearly lower in energy than **M3a**. There are no Cu−C(N) contacts in **M3d** and **M3e**; the calculated Cu−C(N) distances are 3.426 Å (**M3d**) and 3.432 Å (**M3e**). The C_s symmetric forms **M3b, M3c**, and **M3f** are not minima on the potential energy surface.

We also calculated isomeric forms of $Me_2Cu(CN)Li_2$ with a tricoordinate Cu **M4**. Structure **M4a** with a linear CuCNLi moiety is a minimum on the potential energy surface. The isomeric form **M4b** is a transition state. Isomeric forms of **M4** with the Li atom bridging the cyano moiety could not be located as minima on the potential energy surface. It should be noted that the calculated Cu−nearest neighbor distance is 2.036 Å for **M4a** and 2.048 Å for **M4b**, which is clearly longer than the calculated average Cu−C distance for the two-coordinated isomers. The most important result, however, is that the isomeric structures with tricoordinate Cu **M4a** and **M4b** are much higher in energy than the isomers with dicoordinate Cu **M3**.

We studied theoretically the influence of a solvent upon the structures and relative energies of the isomeric forms of $Me_2Cu(CN)Li_2$. To this end, the geometries of various isomers where each Li atom is coordinated by one water molecule have been optimized. Figure 6 shows the optimized geometries of **M5a**−**M5d**, which are related to **M3b**−**M3e**. The calculations predict that the relative energies of the unsolvated isomers **M3b**−**M3e** change very little when two water molecules are added. Structures **M5c** and **M5d** are lower in energy than **M5a** and **M5b**. Although we could not calculate the vibrational frequencies of the isomers **M5a**−**M5d**, we think that **M5c** and **M5d** are probably minima on the potential energy surface, while **M5a** and **M5b** are not.

We also calculated isomers of **M5** where the dicoordinate Cu is bound to the cyano group. Figure 6 shows the optimized geometries of **M6a** and **M6b**. Both structures are clearly higher in energy than the isomeric forms **M5c** and **M5d**. Figure 6 shows also the optimized geometry of **M7**, which has a tricoordinate copper atom. Structure **M7** is related to the

(53) Snyder, J. P.; Spangler, D. P.; Behling, J. R.; Rossiter, B. E. *J. Org. Chem.* **1994**, *59*, 2665−2667.
(54) Bertz, S. H.; Snyder, J. P. *Organometallics* **1995**, *14*, 1213−1220.
(55) Schleyer, P. v. R.; Sawaryn, A.; Reed, A. E.; Hobza, P. *J. Comput. Chem.* **1980**, *7*, 666.

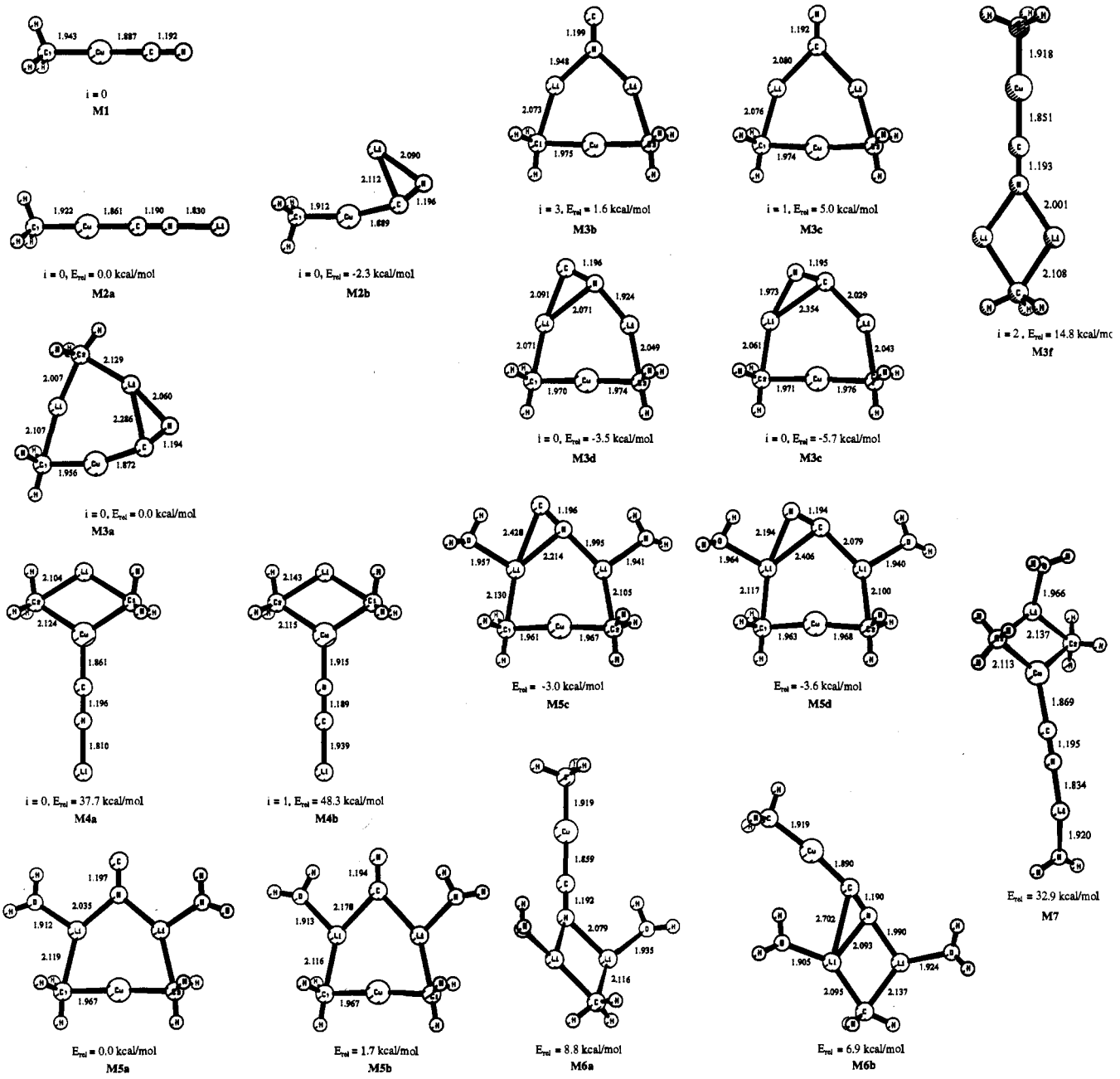

Figure 6. Optimized geometries at MP2/II for compounds **M1**−**M7**. Interatomic distances given in Å. The number of imaginary frequencies is given as i ($i = 0$ indicates an energy minimum, $i = 1$ indicates a transition state, and $i > 1$ indicates a higher order saddle point). Relative energies E_{rel} are given in kcal mol^{-1}.

unsolvated forms **M4a** and **M4a**. The addition of two water molecules to the Li atoms of the latter forms has little effect upon the relative energies. Structure **M7** is much higher in energy than the isomeric forms **M5c** and **M5d**.

Discussion

The observation of nearly identical pre-edge transitions for **2** and **3** suggests that the Cu ions in these solutions possess similar geometries. In particular, the intensity of the pre-edge transition is most consistent with linear, two-coordinate Cu(I) in both solutions. The intensity of the pre-edge feature is somewhat lower for **1**, suggesting that the Cu in this solution may be slightly closer to a three-coordinate geometry. However, the pre-edge intensity in **1** is substantially larger than that seen in authentic three-coordinate Cu(I) complexes. This may indicate that **1** contains a mixture of two- and three-coordinate Cu sites. The intensity of the continuum resonance at approximately 8995 eV decreases as BuLi is added. It is difficult to interpret this change quantitatively. However, the 8995 eV transition appears to be associated with the multiple scattering from linear CN^- groups. This transition is intense for CuCN (s) and $Zn(CN)_2$ (s), consistent with the presence of ca. two and four cyanide ligands, respectively, per metal. The progressive loss of intensity from **1** to **2** to **3** suggests the progressive replacement of cyanide by other, nonmultiple-scattering, ligands as BuLi is added.

Solid and Solution Structure of CuCN. The Fourier transforms for **1,** CuCN (s), and $Zn(CN)_2$ (s) are similar, suggesting similar structures (see Figures 3 and 4). The structure of $Zn(CN)_2$ is known[38] to consist of tetrahedral Zn atoms with linearly bridging cyanide linkages (Zn−C≡N−Zn). Although CuCN has not been characterized crystallographically, it is believed to exist as a polymer with similar Cu−C≡N−Cu units.[38] On the basis of the EXAFS data, the solubilized CuCN

in **1** (CuCN·2LiCl) appears to contain a similar, oligomeric structure. One potential explanation for the observation of Cu···Cu scattering in **1** would be the precipitation of a fraction of Cu in **1** as solid CuCN. On the basis of the amplitude of the third peak in the Fourier transform, nearly 50% of the Cu in **1** would have to be present as CuCN(s) in order to account for the observed EXAFS. In contrast, we observed no evidence for precipitation and the solution remained clear on freezing. A second line of evidence demonstrating that CuCN (s) does not account for the Cu···Cu peak in **1** is the observation that the apparent Cu···Cu distance changes significantly between CuCN (s) and **1**.

On the basis of these observations, we conclude that the LiCl solubilized form of CuCN contains a previously unanticipated oligomeric $[\cdots Cu-C\equiv N-\cdots]_n$ structure in THF solution. The crystal chemistry of Cu(I) cyanides is replete with examples of $[Cu(CN)]_n$ units,[56] including $[Cu(CN)]_3$ rings in catena($(\mu^2$-cyano)-1,10 phenanthrolinecopper(I))[57] and $[Cu(CN)]_6$ rings in $K[Cu_2(CN)_3]$.[58] We are not aware of previous suggestions that these units persist in solution; however, it appears likely that an analogous structure has been solubilized to form **1**. The existence of such units in solution may be important in the assembly of metal cyanide structures.[38]

It is difficult to determine coordination numbers accurately using EXAFS, and typical uncertainties are ±25%. The best integer nearest neighbor coordination number for CuCN (s) is 2, while that for **1** is between 2 and 3, suggesting that there is an increase in the average Cu coordination number when CuCN is dissolved in THF. The average nearest neighbor bond lengths are consistent with an increase in Cu coordination number. The average Cu−nearest neighbor bond length in CuCN (s) is ~1.86 Å, and this increases by ~0.11 Å on formation of **1**. The 1.86 Å distance is consistent with the average Cu−C and Cu−N distances found for two-coordinate Cu,[59,60] although there are few crystallographically characterized two-coordinate Cu cyanides available for comparison. Three-coordinate Cu cyanides are far more common. For these, the average Cu−(C/N) distance is ~1.92 Å.[61] The increased Cu−(C/N) distance in **1** is thus consistent with an increase in Cu coordination number. As noted above, this increase may come in part from halide ligation, as suggested by the presence of Cu−Cl scattering in the EXAFS for **1**. Alternatively, it is possible that solvent is coordinated to some of the Cu ions. In this case, the average of longer $Cu-O_{THF}$ distances and shorter Cu−CN distances would contribute to the increase in the average Cu−nearest distance. It is not possible with the present data to resolve the different contributions to the first shell EXAFS, and thus, it is difficult to distinguish between these structural possibilities. However, the observation of outer shell Cu···N scattering provides additional information to distinguish between possible structures. In particular, the Cu···N distance increases by only ~0.05 Å between CuCN (s) and **1**, despite the 0.11 Å increase in the average nearest neighbor distance. If the average C−N distance is unchanged, the average $Cu-C_{cyanide}$ distance in **1** must be approximately 0.05 Å longer than that in CuCN (s), i.e., ~1.91 Å. Since the average Cu−nearest neighbor distance in **1** is ~0.06 Å longer than this, there must be additional ligation in **1** at distances ≥~2.05 Å. This would be consistent with coordination of THF to some of the Cu(I) ion. A similar structural model is reached if the C−N distance is taken as 1.15 Å, the average value for crystallographically characterized Cu cyanides,[61] and the EXAFS derived Cu···N distance is used to calculate the Cu−C distances. In this case, the apparent $Cu-C_{cyanide}$ bond length is ca. 3.05−1.15 = 1.90 Å.

It is difficult to define the Cu coordination sphere in **1** more precisely, since the Cu−X (X = O_{THF}, Cl, C, and/or N) distance that is necessary to give an *average* first shell distance of ca. 1.97 Å will depend on the ratio of cyanide:X ligands. In all likelihood, there are a variety of different Cu environments, which are averaged to give the observed EXAFS.

Regardless of the details of the Cu−X ligation, it is clear that the average Cu must be coordinated to approximately two cyanides in order to account for the intensity of the Cu···N peak. Since the Cu^+:CN^- stoichiometry in **1** is 1:1, each Cu can only be coordinated to approximately two cyanides if most of the cyanides are bridging between two Cu(I) ions. Virtually all of the crystallographically characterized examples of cyanide bridges between Cu(I) ions involve nearly linear Cu−C≡N−Cu structures.[56] Consequently, it is not surprising that **1** shows a Cu···Cu feature similar to that in CuCN (s). The somewhat lower amplitude of the Cu···Cu peak in **1** relative to CuCN (s) may be due either to a decrease in the number of Cu···Cu interactions or to an increase in the disorder in the Cu···Cu peak (e.g., as a result of bending within the Cu−C≡N−Cu unit). Overall, however, the Cu−C≡N−Cu geometry must remain nearly linear in **1**, since any significant deviations from linearity would result in significant damping of the outer peaks together with errors in the apparent Cu···N and Cu···Cu distances.

For a linear Cu−C≡N−Cu geometry, the difference between the Cu···Cu distance and the Cu···N distance should give the average Cu−(C/N) nearest neighbor distance. The differences are 1.85−1.86 Å for CuCN (s) and 1.92−1.94 Å for **1**, in excellent agreement with the Cu−(C/N) nearest neighbor distances deduced from the Cu···N distance alone, and, for CuCN(s), with the apparent Cu−(CN) distance found from analysis of the first shell EXAFS. The self-consistency of these results is remarkable given the difficulty of determining accurate outer shell distances in EXAFS. The good internal agreement of the fitting results suggests that our model of linear Cu−C≡N−Cu interactions is a good description of these structures.

Solution Structure of 1:1 BuLi + CuCN. The most dramatic differences between **1** and **2** are the absence of the Cu···Cu peak and the decrease in the amplitude of the Cu···N peak in **2**. The Cu···N peak in **2** is approximately half as large as that in **1** or CuCN (s), and is well modeled by approximately one cyanide per Cu. This suggests that the butyl group in **2** has displaced one of the cyanide ligands on the Cu, in agreement with the decrease in cyanide coordination that was indicated by the decrease in continuum resonance intensity in the XANES. The lack of a Cu···Cu EXAFS feature in **2** demonstrates that the oligomeric structure in **1** has been disrupted by the addition of a butyl group. There appear to be few or no Cu−C≡N−Cu bridges in **2**, as expected if there is an average of ca. 1 cyanide coordinated per copper.

The average nearest neighbor distance for **2** is approximately 1.90 Å with an apparent coordination number of two. This bond length is too short to be consistent with a three-coordinate Cu

(56) Hathaway, B. J. In *Comprehensive Coordination Chemistry*; Wilkinson, G., Gillard, R. D., McCleverty, J. A., Eds.; Pergamon: Oxford, 1987; Vol. 5; pp 533−774.

(57) Dyason, J. C.; Healy, P. C.; Engelhardt, L. M.; Pakawatchai, C.; Patrick, V. A.; Ratson, C. L.; White, A. H. *J. Chem. Soc., Dalton Trans.* **1985**, 839.

(58) Roof, R., B.; Larson, A. C.; Cromer, D. T. *Acta Crystallogr., Sect. B* **1968**, *24*, 269.

(59) Peng, S.-M.; Liaw, D.-S. *Inorg. Chim. Acta* **1986**, *113*, L11.

(60) Dessey, G.; Fares, V.; Imperatori, P.; Morpurgo, G. O. *J. Chem. Soc., Dalton Trans.* **1985**, 1285.

(61) The Cambridge Structural Database was searched to identify 37 structures containing bridging Cu(I)−CN−M cyanides and 15 structures containing terminal Cu(I)−CN cyanides. Average C−N distances were 1.15 ± 0.02 Å and 1.14 ± 0.03 Å, respectively. Average Cu−C distance of 1.92 ± 0.03 Å is based on 15 structures having three-coordinate Cu(I) with unambiguous distinction between the C and the N of the cyanide.

but is completely consistent with that expected for [Bu−Cu−CN]⁻. This provides structural confirmation for the [R−Cu−CN]⁻ structure proposed previously on the basis of NMR data.[19] The expected $Cu-C_{cyanide}$ distance for a two-coordinate Cu is approximately 1.85 Å,[59] while the few crystallographically characterized two-coordinate Cu−alkyl complexes have Cu−C bond lengths of approximately 1.95 Å.[20,62] The apparent Cu···N distance is roughly consistent with this structural model, although the agreement is not as good as for **1**. The observed Cu···N distance of ~3.07 Å implies a $Cu-C_{cyanide}$ distance of 1.92 Å, which in turn implies a $Cu-C_{butyl}$ distance of ~1.88 Å in order to give the observed first shell distance. Within the uncertainty of the outer shell EXAFS (± 0.05 Å), these are consistent with the expected distances.

Solution Structure of 2:1 BuLi + CuCN. We have previously noted the absence of detectable outer shell scattering in **3**.[29] This is consistent with the absence of cyanide ligation in these solutions. It is possible that cyanide could be coordinated, giving a three-coordinate Cu, but bent so that outer shell Cu···N scattering was not detectable. However, this is inconsistent with the similarity of the XANES spectrum for **2** and **3**. The 1s → 4p transitions for these solutions have identical amplitudes and energies, indicating that, whatever structural change occurs on addition of the second equivalent of BuLi, it does *not* involve a significant change in the Cu geometry. The only change in the XANES spectra is the decrease in the continuum resonance intensity. This, again, is consistent with loss of the cyanide ligand.

The EXAFS data, with an apparent coordination number of two, provide further support for a two-coordinate Cu in **3**. Although EXAFS data can underestimate coordination numbers if a shell is disordered, the bond length for **3** is too short to be consistent with a three-coordinate Cu. In contrast, the Cu−C bond length in **3** is exactly what would be expected for $[Bu_2Cu]^-$.[20,63] The increase in bond length relative to **2** is consistent with replacing an sp-hybridized cyanide carbon by an sp^3-hybridized butyl carbon.

The XANES and EXAFS for **3** are thus both consistent with a Bu−Cu−Bu structure for the immediate ligation environment of the Cu. The absence of outer shell EXAFS features rules out a linear cyanide ligand, while the 1s → 4p intensity and the average Cu-C bond length rule out copper coordination numbers greater than two. The simulation in Figure 4 suggests that a bent cyanide should give detectable, albeit weaker, long-range scattering in contrast with the absence of outer shell scattering in **3**. The lack of a long range signal cannot, however, prove the absence of outer shell ligands that perhaps cannot be detected as a consequence of thermal disorder or destructive interference. Thus, the EXAFS and XANES data alone do not rule out a structure in which the Cu is coordinated to *one* butyl group and one *bent* cyanide ligand.

Since terminal cyanides are approximately linear, a bent cyanide would imply a μ-1,1-bridging geometry (e.g., M3a). However, both the IR and the NMR properties of the "higher order" cyanocuprates are inconsistent with a μ-1,1-bridging cyanide. The cyanide stretching frequencies would be expected to *decrease* significantly due to significantly increased sp^2 character at the bridging carbon. Although structures of authentic π-bound and μ-1,1-bridging cyanides are rare (only two μ-1,1-cyanide bridged copper complexes have been crystallographically characterized[57,64]), this trend is well documented for the isocyanide and isoelectronic CO complexes. Terminal CO ligands typically appear ca. 200 cm^{-1} higher in energy than μ-1,1 bridging CO's,[65,66] while isocyanide C≡N stretching frequencies decrease by approximately 400 cm^{-1} on going from a terminal to a bridging geometry. In contrast, the reported C≡N stretching frequency of $R_2CuLi{\cdot}Li(CN)$ in THF is slightly *higher* than LiCN in THF.[16,67,68] Similarly, the ^{13}C chemical shifts of the cyanide ligand are expected to move dramatically downfield for a μ-1,1 bridging cyanide. The ^{13}C resonances of μ-1,1 CO ligands appear 50−70 ppm downfield of terminal CO ligands,[65] while μ-1,1 bridging isocyanide ^{13}C chemical shifts appear 90−100 ppm downfield of their terminal counterparts.[65,66,69−73] However, the ^{13}CN chemical shifts reported for cyanide in "higher order" cuprates are shifted only about 5 ppm downfield from "lower order" cyanocuprates.[16,67]

The combination of EXAFS and XANES measurements with IR and NMR results thus rule out both the original "higher-order" cyanocuprate structure, R_2CuCN^{2-}, and a modified structure in which the cyanide is bent. Recently, Lipshutz and James have suggested a third possibility in which the cyanide is π-coordinated to the Cu.[67] This structure is also inconsistent with the EXAFS and XANES for **3**.[74]

There are two final points to consider regarding the EXAFS data. The first concerns the oligomerization state of **2** and **3**. Neither shows the Cu···Cu peaks found in **1**. This does not necessarily mean that the Cu sites in **2** and **3** are monomeric. EXAFS spectra are unlikely to be sensitive to outer shell scattering from weakly coupled, e.g., Li^+ bridged, structures. The second, related, point concerns the location of the cyanide in **3**. Although the XANES and EXAFS data clearly rule out structures in which the CN^- is bound to the Cu, there are several examples of cases in which EXAFS has failed to detect nearest neighbors that interact only weakly with a metal center. Thus, the methionine sulfur at 3.0 Å from the Cu in plastocyanin is not EXAFS detectable.[75] It is impossible to rule out an analogous, extremely weak Cu···CN^- interaction in **3**.

In order to better define the nature of the Cu/CN^- interaction, we undertook theoretical calculations of various possible structures. In general, the bond lengths for the optimized structures, **M2b** and **M5d**, are in remarkably good agreement with the observed EXAFS distances.

The principal conclusion of the theoretical calculations is that the isomeric forms of 2:1 cyanocuprates with a tricoordinate Cu are energetically very unfavorable compared with dicoordinate structures. The dicoordinate forms with a Cu−CN bond are also higher in energy than those isomers which have no Cu−CN bonds. The calculations strongly support the conclu-

(62) Dempsey, D. F.; Girolami, G. S. *Organometallics* **1989**, *7*, 1208.
(63) Dempsey, D. F.; Girolami, G. S. *Organometallics* **1989**, *7*, 1208.
(64) Cromer, D. T.; Larson, A. C.; Roof, R. B. *Acta Crystallogr.* **1965**, *19*, 192.
(65) Ennis, M.; Kumar, R.; Manning, A. R.; Howell, J. A. S.; Mathru, P.; Rowan, A. J.; Stephens, F. S. *J. Chem. Soc., Dalton Trans.* **1981**, 1251−1259.
(66) Benner, L.; Balch, A. S. *J. Am. Chem. Soc.* **1978**, 6106.
(67) Lipshutz, B. H.; James, B. *J. Org. Chem.* **1994**, *59*, 7585.
(68) Singer, R. D.; Oehlschlager, A. C. *J. Org. Chem.* **1992**, *57*, 2192−2195.
(69) Grundy, K. R.; Robertson, K. N. *Organometallics* **1983**, *2*, 1736−1742.
(70) Lin, Y.-W.; Gau, H.-M.; Wen, Y.-S.; Lu, K.-L. *Organometallics* **1992**, *11*, 1445−1447.
(71) Hanson, A. W.; McAlees, A. J.; Taylor, A. *J. Chem. Soc., Perkin Trans. 1* **1985**, 441−446.
(72) Joshi, K. K.; Mills, O. S.; Pauson, P. L.; Shaw, B. W.; Stubbs, W. H. *Chem. Commun.* **1965**, 181−182.
(73) Olmstead, M. M.; Hope, H.; Benner, L. S.; Balch, A., L. *J. Am. Chem. Soc.* **1977**, *99*, 5502−5503.
(74) Barnhart, T. M.; Huang, H.; Penner-Hahn, J. E. *J. Org. Chem.* **1995**, *60*, 4310−4311.
(75) Penner-Hahn, J. E.; Murata, M.; Freeman, H. C.; Hodgson, K. O. *Inorg. Chem.* **1989**, *28*, 1826−1832.

sion from EXAFS spectroscopy that the copper atoms in 2:1 cyanocuprates are not tricoordinate and do not have a close contact to a cyanide ligand.

The butyl group in these solutions appears to be an even better ligand for Cu(I) than is cyanide. Not only does butyl displace one cyanide in **1**, thereby disrupting the oligomeric structure, but the butyl group will also displace the second cyanide from **2** to give a species best formulated at $[Bu_2Cu]^-$ in **3**. The EXAFS measurements and the theoretical calculations both show that CN^- is not coordinated to the Cu in **3**.

There have been numerous spectroscopic studies, primarily NMR and IR, comparing the properties of cuprates formed from halo- and cyanocopper salts.[1,16,18,19,76] These spectroscopic measurements, most recently an elaborate study involving *in situ* generation of LiCN,[67] show unambiguously that the CN^- is in a different environment in **1**, **2**, and **3**. These findings have been interpreted[16,67] as evidence for the existence of a so-called "higher-order" cyanocuprate species, in which the cyanide is coordinated directly to the Cu. It is perhaps more appropriate to conclude that the cyanide environment is *different* in **1**, **2**, and **3**, but not necessarily that the cyanide is coordinated to Cu. The present results strongly suggest that this unique $Cu^+/CN^-/2R^-/2Li^+$ complex has a basic structure similar to that shown in **M3e**. This structure would account for the unique spectroscopic properties of the cyanide in **3**.

What remains unclear, however, is what role CN^- *is* playing in these solutions, i.e., why structures like **M3e** should possess unique reactivity properties. There is a substantial body of literature suggesting that cyanocuprates possess unique reactivity properties in comparison with their halide analogs.[9-14] Possible roles for the cyanide involve interception of impurities and/or side products or stabilization of a subsequent structure that lies further along the reaction pathway. Alternatively, it may be that halides interfere with the formation, stability, or reactivity of organocuprate species; thus, the principal advantage of cyanide would be that it is not a halide. Experiments designed to test these possibilities are in progress.

Acknowledgment. SSRL and NSLS are supported by the U.S. Department of Energy. SSRL and beamline X-9A are supported by NIH Research Resource grants. J.E.P.H. was supported in part by a grant from the A. P. Sloan Foundation and T.M.B. by a fellowship from the Herman and Margaret Sokol Foundation. P.K. and G.F. thank the Deutsche Forschungsgemeinschaft (SFB 260 and Graduiertenkolleg Metallorganische Chemie) for financial support. The authors wish to thank Professor Ninian Blackburn for EXAFS data on $Cu(CN)_3^{2-}$ and Mr. Hui Huang for the $NaCu(CN)_2 \cdot 2H_2O$ data.

JA951598R

(76) Bertz, S. H.; Dabbagh, G.; He, X.; Power, P. P. *J. Am. Chem. Soc.* **1993**, *115*, 11640.